Analytical Solution for the Integral Contact Line Evaporative Heat Sink

J. A. Schonberg* and P. C. Wayner Jr.†
Rensselaer Polytechnic Institute, Troy, New York 12180

Heat transfer by evaporation from a thin film is studied theoretically. The film thickness decreases with position and approaches an asymptotic value. The film is influenced by long-range intermolecular forces, in particular van der Waals forces. According to the model, as well as previous models, these forces may partially suppress evaporation, locally, but may draw fluid into the thin film from a bulk pool, generally. The insulation effect of the fluid is included, whereas, capillary and thermocapillary effects are not considered. Analytical expressions are presented for the film slope, curvature, and flow in terms of the film thickness. The film is semi-infinite and steady, therefore, the flow at some position is equal to evaporation from the portion of the film downstream of that position and is proportional to the integral heat sink. Curvature may become quite large for small film thicknesses. An expression for the film thickness as a function of position is presented for the special case of a relatively strong insulation effect. Also presented is an engineering model relating the integral heat sink to a reduction in the Laplace pressure driving force for porous media flow, through a dynamic contact angle.

Nomenclature

A = Hamaker constant ($6\pi\bar{A}$)
a, b = functions of bulk properties
B = disjoining pressure constant
C_1 = condensation coefficient
d = pore diameter
h = enthalpy, heat transfer coefficient
K = curvature
k = thermal conductivity of the liquid
M = molecular weight
$\dot{M}$ = dimensionless evaporative flux
$\dot{m}$ = interfacial mass flux
n = an integer
P = pressure
Q = integral heat sink
q = the evaporative heat flux
R = gas constant
T = temperature
u = transformed η defined by equation (24)
V = molar volume
W = a mathematical convenience
x = distance along substrate surface
Γ = mass flow rate/width
γ = interfacial tension
Δ = difference
δ = film thickness
η = dimensionless thickness
θ = contact angle
λ = dimensionless group defined in Eq. (11)
μ = dynamic viscosity
ν = kinematic viscosity
ξ = dimensionless position
Π = disjoining pressure
ρ = density

Subscripts
e = effective
i = average value
l = liquid
lv = liquid-vapor interface
m = unit mass
0 = reference value
s = substrate
t = total, referring to entire thin film
v = vapor
x = at x

Superscripts
id = ideal
$', ''$ = derivatives
$*$ = dimensionless quantity symbols
$<<$ = much less than

Introduction

EVAPORATION in the contact line region of an evaporating thin film (junction of vapor, evaporating thin film, and adsorbed nonevaporating thin film on a solid substrate) is important in many change of phase heat transfer processes. For example, the stability of a steady-state evaporating meniscus depends on the physicochemical phenomena occurring in this region. Due to the difficulties associated with experimentation in a small region where the film thickness becomes very thin, analytical descriptions of the transport processes are indispensable. Herein, we focus on an analytical description of the critical leading edge of an evaporating film. Due to the short conduction path associated with ultra-thin films, large heat fluxes are possible. However, it is not obvious how or if the potential of the thin film may be harnessed to provide high-heat fluxes. Higher heat flux processes are more complicated; for example, experimental evidence shows that in some systems evaporating thin films become unsteady at higher heat fluxes. Therefore, the model presented herein is not intended to be a complete description of high-heat flux processes but is an attempt to describe some of their essentials.

Very thin films on solid substrates are subject to long-range intermolecular forces which affect their vapor pressure and, therefore, their tendency to evaporate. In fact, experiments reported by Derjaguin and Zorin[1] show that a thin film of a completely wetting fluid persists at equilibrium with its sat-

Received July 16, 1990; revision received Oct. 24, 1990; accepted for publication Oct. 25, 1990.

*Research Associate, Howard Isermann Department of Chemical Engineering.
†Professor of Chemical Engineering, Howard Isermann Department of Chemical Engineering.

urated vapor even though it is superheated. Furthermore, feeding fresh liquid to a nonequilibrium thin film involves large pressure gradients due to high shear stresses. These two concepts are connected at the molecular level because they both depend on the intermolecular force field. For example, if the liquid film has a large negative pressure due to viscous shear, the free energy may be so reduced that evaporation is seriously hindered. Other complications in evaporating thin films involve surface tension, e.g., capillary pressure and Marangoni flow.

Inspite of these complications, the evaporating thin film has received attention over the years. Various works by Derjaguin et al.,[2] Potash and Wayner,[3] Miller,[4] Wayner et al.,[5] Holm and Goplen,[6] Moosman and Homsy,[7] Parks and Wayner,[8] Mirzamoghadam and Catton,[9] and Das and Gaddis[10] are briefly reviewed in Wayner and Schonberg.[11] A related paper on the nonlinear stability of evaporating/condensing liquid films was published by Burelbach et al.[12]

This work is an extension of Wayner et al.[5] In that study evaporation from a steady thin film was related to the bulk thermodynamic properties of the liquid, the superheat, the fluid viscosity, and the disjoining pressure. Capillary and conductivity effects were not treated. The liquid was taken to have a simple form of disjoining pressure.

$$P_v - P_l = -\frac{\bar{A}}{\delta^3} \tag{1}$$

where P_v is the pressure in the vapor phase, P_l is the pressure in the liquid phase, $\bar{A}$ is a negative constant, and δ is the thickness of the film.

The disjoining pressure is a pressure difference across the liquid vapor interface due to a repulsion of the vapor phase by the solid and the liquid, due to long-range intermolecular forces, in this case van der Waals forces. The film was taken to be fairly flat so that its hydrodynamics are described by lubrication theory. Finally, an expression was developed to relate the evaporative flux to the superheat of the liquid **and** to the pressure of the liquid. A second-order ordinary differential equation was developed and solved numerically for the film thickness profile as well as the amount of power absorbed by the evaporating thin film. This total power, which is not a flux, but is the power per unit length of contact line for a specified portion of the thin film, is defined as the integral contact line evaporative heat sink. The term "contact line" refers to the junction of a meniscus and a nonevaporating thin film (of course, the junction is a smooth transition). In this work we present an analytical solution for the integral contact line evaporative heat sink including film conductivity effects. Furthermore an analytical film profile is presented for the case of strong conductivity effects. As in the work of Wayner et al.[5] capillary and Marangoni effects are ignored, however, the importance of capillary effects is discussed. The numerical example gives significant insight concerning the characteristics of the heat transfer process near the contact line. In comparison to a recent paper by Wayner[12] in which both the thickness and slope were arbitrarily selected, only the thickness needs to be specified. As a result, higher fluxes in the contact-line region can be envisioned within the assumptions associated with the analysis.

Review of the Thin Film Model

Consider the thin film of pure liquid illustrated in Fig. 1. The vapor phase is pure as well. Based on kinetic theory, the mass flux of vapor leaving the liquid vapor interface, $\dot{m}$, is modeled as

$$\dot{m} = a(T_{lv} - T_v) + b(P_l - P_v) \tag{2}$$

where T_{lv} is the temperature of the liquid at the liquid vapor interface, T_v is the temperature of the vapor phase, P_l is the pressure of the liquid, and P_v is the pressure of the vapor phase. The vapor phase is assumed to have a uniform pressure

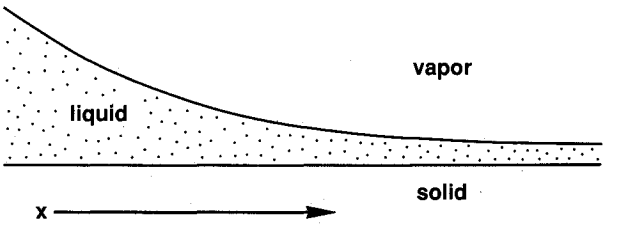

Fig. 1 Evaporating thin film and coordinate system.

and temperature. Furthermore, it is assumed to be in equilibrium with the **bulk** liquid at temperature T_v. The resistance to transport in the vapor phase in the actual process is ignored in the model. Equation (2) is a condensed form of Eqs. (10), (13), and (19) given in Wayner et al.[5] which was an extension of the mass effusion model of Schrage.[13] In Eq. (2) the effect of liquid pressure and temperature on the vapor pressure, and therefore, the mass flux, is modeled. The coefficients a and b are functions of the bulk properties of the liquid. The coefficients are

$$a = C_1 \left(\frac{M}{2\pi R T_{lv}}\right)^{1/2} \left(\frac{P_v M \Delta h_m}{R T_v T_{lv}}\right) \tag{3}$$

and

$$b = C_1 \left(\frac{M}{2\pi R T_{lv}}\right)^{1/2} \left(\frac{V_l P_v}{R T_{lv}}\right) \tag{4}$$

where, taking the accommodation coefficient equal to one, we assign

$$C_1 = 2.0 \tag{5}$$

and where M is the molecular weight, R is the universal gas constant, Δh_m is the enthalpy of vaporization, and V_l is the molar volume of the liquid. The functions "a" and "b" are not sensitive to small changes in T_v and T_{lv}, therefore, these quantities may be replaced with the substrate temperature provided the temperature differences are small.

The evaporative heat flux, q, is

$$q = \dot{m} \Delta h_m \tag{6}$$

Equation (2) states that the interfacial mass flux is affected by a difference in the temperature and pressure across the interface. In this model, the resistance associated with the dynamic mass transfer processes in the vicinity of the interface is confined to the interface. For a thin, flat, completely wetting film, the effective liquid phase pressure is below the vapor phase pressure because of the solid-liquid-vapor interfacial force field. Now the vapor phase is in thermodynamic equilibrium with bulk liquid. Therefore, the total pressure of the liquid thin film is below that of the bulk liquid. Hence, the vapor pressure of the liquid thin film is less than the vapor pressure of the bulk liquid in the absence of a temperature difference. If the temperature of the film at the liquid vapor interface exceeds the temperature of the vapor phase, this effect is offset. The increase of vapor pressure with temperature is a familiar concept. Only if that temperature difference is sufficient will evaporation occur. This is, generally speaking, the reverse of what occurs in an evaporating drop of liquid.

As in the analysis of Moosman and Homsy,[7] the temperature of the liquid, at the liquid vapor interface, is related to the temperature of the substrate, T_s, through the one-dimensional conduction heat transfer model for the liquid film

$$\dot{m} = \frac{k}{\delta \Delta h_m} (T_s - T_{lv}) \tag{7}$$

where k is the thermal conductivity of the liquid. Equations (2) and (7) may be combined to eliminate T_{lv} in favor of T_s to obtain

$$\dot{m} = \left(1 + \frac{a\delta\Delta h_m}{k}\right)^{-1} (a(T_s - T_v) + b(P_l - P_v)) \quad (8)$$

The temperature difference is a constant, ΔT,

$$\Delta T \equiv T_s - T_v \quad (9)$$

and is the immediate cause of the evaporation process. The pressure change at the liquid vapor interface is, in general, given by

$$P_v - P_l = \frac{-B}{\delta^n} + \gamma K \quad (10)$$

where K is the curvature of the interface, and γ is the surface tension. For a completely spreading fluid $B < 0$ and, therefore, $P_l < P_v$. The reduction in vapor pressure due to this pressure jump is offset by the temperature jump to give evaporation. We restrict our attention to very thin films with low curvature and use Eq. (1). In essence, we are emphasizing the region in the immediate vicinity of the contact line which stabilizes the liquid film. Using Eq. (1) and the dimensionless group

$$\lambda \equiv \frac{a\Delta h_m \delta_0}{k} \quad (11)$$

we find

$$\dot{m} = \frac{1}{1 + \lambda\delta/\delta_0}\left(a\Delta T + \frac{b\bar{A}}{\delta^3}\right) \quad (12)$$

If δ is small enough there is no evaporative flux. This value of δ is the reference thickness and is given by

$$\delta_0 = \left(-\frac{b\bar{A}}{a\Delta T}\right)^{1/3} \quad (13)$$

With this reference thickness Eq. (12) may be scaled to yield the dimensionless flux $\dot{M}$,

$$\dot{M} = \frac{\dot{m}}{\dot{m}^{id}} = \frac{1}{1 + \lambda\eta}\left(1 - \frac{1}{\eta^3}\right) \quad (14)$$

where η is the dimensionless thickness

$$\eta = \frac{\delta}{\delta_0} \quad (15)$$

The reference flux $\dot{m}^{id}$ is the flux that would occur in the absence of pressure effects

$$\dot{m}^{id} = a\Delta T = -b\bar{A}\delta_0^{-3} \quad (16)$$

To summarize, the literature provides a model relating the local evaporative flux to the local film pressure and interfacial temperature change. The interfacial temperature change is related to the temperature difference between the solid and vapor phases, the film thickness, and the local evaporation rate. The local film pressure is related to the local film thickness. Therefore, a particular thin film shape (profile) has a corresponding evaporative flux profile. However, mass is conserved and there must be a corresponding flow. The flow of a thin film is described by lubrication theory and the continuum assumption.

Lubrication theory relates the mass flow in the thin film, Γ, to the pressure gradient in the direction of flow

$$\Gamma = -\frac{\delta^3}{3\nu}\frac{dP_l}{dx} \quad (17)$$

where ν is the kinematic viscosity. The coordinate x is the distance in the direction of flow and is pictured in Fig. 1. Using Eq. (1) in Eq. (17) gives

$$\Gamma = \frac{\bar{A}}{\nu}\frac{1}{\delta}\frac{d\delta}{dx} \quad (18)$$

For a steady evaporating thin film, a mass balance implies

$$\dot{m} = -\frac{\bar{A}}{\nu}\frac{d}{dx}\left(\frac{1}{\delta}\frac{d\delta}{dx}\right) \quad (19)$$

Equation (19) is made nondimensional using Eq. (15) and the relationship

$$\xi = \frac{x}{x_0} \quad (20)$$

where

$$x_0^2 \equiv \frac{-\bar{A}}{\nu\dot{m}^{id}} \quad (21)$$

Therefore, the local evaporative flux is related to the thin film shape (profile) through lubrication theory

$$\dot{M} = \frac{d}{d\xi}\left(\frac{1}{\eta}\frac{d\eta}{d\xi}\right) \quad (22)$$

Therefore, a steady thin film has the shape needed to induce a specific evaporation flux profile and to induce the pressure profile needed to pump liquid to support the evaporation. In mathematical terms, we have from Eqs. (14) and (22) the expression

$$\frac{d}{d\xi}\left(\frac{1}{\eta}\frac{d\eta}{d\xi}\right) = \frac{1}{(1 + \lambda\eta)}\left(1 - \frac{1}{\eta^3}\right) \quad (23)$$

Having discussed the development of the differential Eq. (23), we now turn our attention to the boundary conditions of interest in this study. The boundary condition is really a far-field condition. The thin film is a transition between a thicker body and a nonevaporating thin film [a film of thickness δ_0 as given in Eq. (13)]. Therefore, the scaled thickness, η, satisfies the limit

$$\eta \to 1$$

as

$$\xi \to \infty$$

Furthermore the slope satisfies the limit

$$\frac{d\eta}{d\xi} \to 0$$

as

$$\xi \to \infty$$

Analytical Solution for Heat Sink

In the previous section, the model of Wayner et al.[5] was reviewed. The extension of Moosman and Homsy[7] to include

the resistance to conduction in the film was reviewed as well. In this section a proposed analytical partial solution of the resulting governing equation is presented.

The governing Eq. (23) is subjected to transformation. We define the variable

$$u = \eta^3 \tag{24}$$

and find from Eq. (23) that

$$\frac{1}{3}\frac{d}{d\xi}\left(\frac{1}{u}\frac{du}{d\xi}\right) = \frac{1}{1 + \lambda u^{1/3}}\left(1 - \frac{1}{u}\right) \tag{25}$$

This equation is invariant with respect to translation in the independent variable ξ, therefore, following Bluman and Cole,[13] the transformation

$$W = \frac{du}{d\xi} \tag{26}$$

is used with the chain rule to eliminate ξ from the equation. The result is a first-order differential equation which may be integrated. The proposed solution is, after back transformation to replace u with η, and inclusion of the farfield condition

$$-\frac{W}{u} = \left[18(1 + \lambda^3)\ \text{fm}\left(\frac{\eta}{1 + \lambda\eta}(1 + \lambda)\right) + 6(\eta^{-3} - 1) + 9\lambda(1 - \eta^{-2}) + 18\lambda^2(\eta^{-1} - 1)\right]^{1/2} \tag{27}$$

The integral heat sink for the contact line region is directly related to this quantity,

$$Q = \Gamma\Delta h_m = \frac{\bar{A}\Delta h_m}{3\nu x_0}\cdot\frac{W}{u} \tag{28}$$

Therefore, W/u is a dimensionless contact line heat sink, Q^*,

$$Q^* \equiv -\frac{W}{u}$$

The solution is discussed in more depth in Appendix A.

Solution for Meniscus Profile and Heat Sink for Zero λ and Larger η

Equation (27) represents a first-order differential equation that we have integrated for a special case. The equation is simplified in that λ has been assumed to be zero (no insulation effects). It is further simplified by assuming that η is large. Specifically we assume

$$\eta^{-3} << 1 \tag{29}$$

Then Eq. (27) becomes

$$-\frac{W}{u} = (18\ \text{fm}\,\eta - 6)^{1/2} \tag{30}$$

solution of this is

$$\eta = e^{1/3}e^{\xi^2/2} \tag{31}$$

We find the film slope to be

$$\frac{d\eta}{d\xi} = \frac{1}{3}\frac{W}{u}\exp\left(\frac{1}{18}\left(\frac{W}{u}\right)^2 + \frac{1}{3}\right) \tag{32}$$

Equation (23) was treated directly by a numerical method for zero λ by Wayner et al.[5]

Solution for Meniscus Profile and Heat Sink for Large λ

The meniscus profile might be found by integrating Eqs. (26) and (27). We propose an analytical solution valid for large λ. Analysis of both Eqs. (27) and (A-10) for the case of large values of λ yields

$$-\frac{1}{\eta}\frac{d\eta}{d\xi} = \lambda^{-1/2}\sqrt{2}\left(1 - \frac{1}{\eta} - \frac{1}{4}\left(1 - \frac{1}{\eta^4}\right)\right)^{1/2} \tag{33}$$

Integration yields

$$\frac{1}{\sqrt{3}}\ \text{fm}\left(\eta + \frac{1}{3} + \sqrt{\left(\eta + \frac{1}{3}\right)^2 + \frac{2}{9}}\right) - \frac{1}{\sqrt{6}}\ \text{fm}\left(\frac{2\eta + 1}{3\eta - 3} + \sqrt{\left(\frac{2\eta + 1}{3\eta - 3}\right)^2 + \frac{1}{18}}\right) = -\frac{1}{\sqrt{2\lambda}}\xi \tag{34}$$

The integral heat sink is, in this case

$$Q = \frac{-\bar{A}\Delta h_m}{\nu x_0}\sqrt{\frac{2}{\lambda}}\left(1 - \frac{1}{\eta} - \frac{1}{4}\left(1 - \frac{1}{\eta^4}\right)\right)^{1/2} \tag{35}$$

The maximum integral heat sink is the heat absorbed by the entire meniscus, Q_t. This is found from Eq. (35) with η "equal" infinity. In dimensional terms

$$Q_t = \sqrt{\frac{3}{2}}(-\bar{A})^{1/3}\left(\frac{\Delta h_m k}{\nu}\right)^{1/2}\left(\frac{a}{b}\right)^{1/6}\Delta T^{2/3} \tag{36}$$

Discussion

The expression for the integral heat sink, Eq. (28), implies that the slope and curvature of the film at some position along the substrate are functions of the amount of heat absorbed by the portion of the meniscus "downstream" of that position, or in other words the amount of material flowing by that position multiplied by the heat of vaporization. The expression for curvature is developed by expanding the left-hand side of Eq. (23) and using the expression for the integral heat sink which provides the slope of the film. That is

$$\frac{1}{\eta}\frac{d^2\eta}{d\xi^2} - \frac{1}{\eta^2}\left(\frac{d\eta}{d\xi}\right)^2 = \frac{1}{1 + \lambda\eta}\left(1 - \frac{1}{\eta^3}\right) \tag{37}$$

The relationship between slope, curvature, and the integral heat sink may be illustrated by a case study.

Consider the system of *n*-octane, silicon, and air. The temperature is 70° C and the temperature difference between the solid and vapor phases is 5.3 (10^{-3})° C. The constant $-\bar{A}$ is found from Truong and Wayner[14] as

$$\bar{A} = -3.18\ (10^{-21})J \tag{38}$$

Based on this information and the physical properties of bulk *n*-octane; the vapor pressure, P_v; the molar volume, V_l; the enthalpy of vaporization, Δh_m; and the kinematic viscosity, ν

$$P_v = 119.03\ \text{Torr}$$

$$V_l = 1.724\ (10^{-4})\ \text{m}^3/\text{mole}$$

$$\Delta h_m = 339.8\ \text{kJ/kg}$$

$$\nu = 4.916\ (10^{-7})\ \text{m}^2/\text{s}$$

we find

$$\delta_0 = 45.08 \text{ Å}$$
$$x_0 = 1962 \text{ Å}$$
$$\lambda = 0.041 \quad (39)$$

Figure 2 provides a plot of $d\delta/dx$ and $d^2\delta/dx^2$ vs the integral heat sink Q, that is given by Eq. (28). Note the only factor in Q that is varied is the dimensionless film thickness η. This plot shows that the slope is steeper and the curvature larger in the portions of the meniscus which experience a greater flow. Curiously, these curves follow one another quite closely. The plot of curvature is important because capillarity is neglected in this analysis. Figure 2 indicates that curvature increases with Q. Therefore, the expression for the integral heat sink may be invalid for the larger values of Q. These values correspond to the thicker portions of the meniscus. The criteria for neglecting capillary pressure is

$$\gamma \frac{d^2\delta}{dx^2} \ll -\frac{\bar{A}}{\delta^3} \quad (40)$$

Taking the surface tension to be 16.87×10^{-3} N/m and using Eqs. (27) and (37) as well as the reference quantities, we estimate the disjoining pressure to be about 10 times larger than the capillary pressure at a thickness of $\eta = 1.25$. For convenience λ is set equal to zero. This corresponds to $Q^* = 1.04$ (or with $\delta T = 4.5$ K, $\delta_0 = 1$ nm, $Q^* = 1.98$). A more indepth treatment of capillary effects and the region of the meniscus over which they are negligible is provided in Schonberg and Wayner.[17] We note that curvature in this example reaches $\delta'' = 700{,}000 \text{ m}^{-1}$ in the region where δ varies between 45 Å and 126 Å. This demonstrates how the curvature builds up near the contact line. Although the small scale of the analyzed region precludes quantitative comparison with experimental data at the present time, the results qualitatively agree with experimental observations in the thicker region.[18]

The heat flux, q, absorbed by an evaporating meniscus is of interest as well. This may be estimated with the ideal evaporation rate, $\dot{m}^{id}$

$$q \approx \dot{m}^{id} \Delta h_m \quad (41)$$

This is illustrated with more case studies. Case 1 corresponds to the conditions listed above, with varying temperature difference, ΔT. Case 2 is the n-octane-silicon-air system at 170° C. The higher temperature has a strong effect on the vapor pressure of n-octane. At 170° C, it is very near 3 atm, whereas at 70° C, it is only 0.16 atm. The ideal heat flux is plotted against ΔT in Fig. 3. The flux is very high, however, it is not yet apparent how or if these fluxes may be realized.

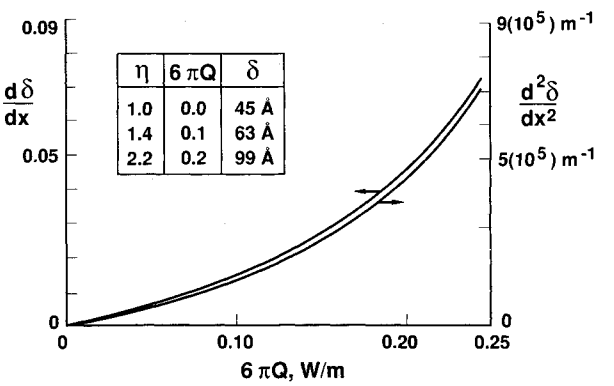

Fig. 2 Absolute value of the film slope and curvature as a function of heat sink for a particular case. Table provides corresponding film thicknesses.

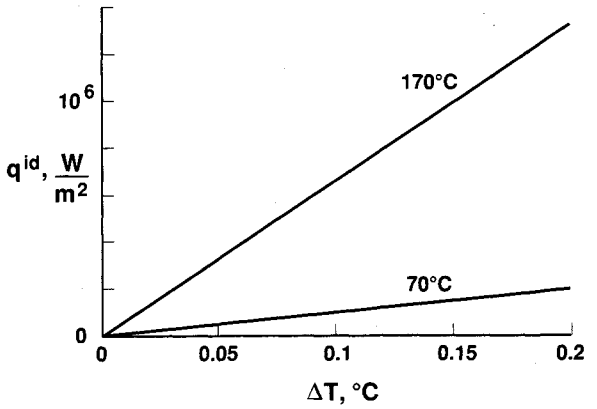

Fig. 3 Ideal heat flux vs solid to vapor temperature change at 70° C and 170° C.

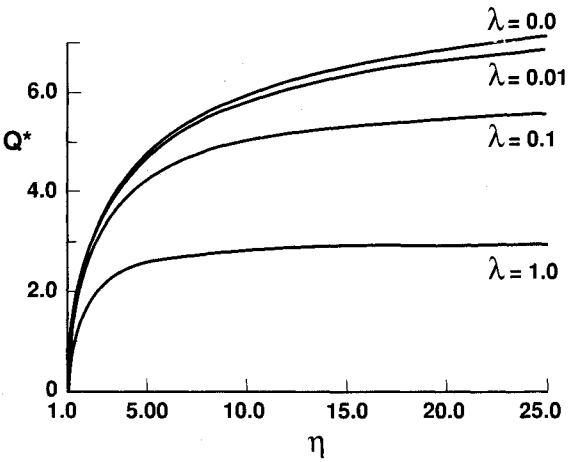

Fig. 4 Integral heat sink vs film thickness for several values of λ.

A dimensionless plot of the integral heat sink vs the film thickness, constructed from Eq. (27), is shown in Fig. 4 for four values of λ. This plot shows that the most active part of the meniscus is the thinnest part, especially for large values of λ. Even though the heat flux decreases as $\eta \to 1$, the area is large because $\eta' \to 0$. Furthermore the resistance to heat transfer by the film is less in the thinnest part.

For large values of λ an analytical expression for the meniscus shape was developed. This is plotted in Fig. 5. Note that the independent variable is $\xi/\sqrt{2\lambda}$. In the numerical solution of Wayner et al., the independent variable is ξ. Therefore, the effect of large resistance in the film (resistance to thermal conduction) is to stretch out the contact-line region. A stronger effect induces more stretching.

For the limiting case of a large λ value, the maximum integral heat sink was found for a thin film. This is given in Eq. (36). The maximum integral heat sink is the total heat absorbed in the contact line region. In the derivation of Eq. (36) capillary effects were neglected. However, this expression may still be valid because, as previously discussed, the thinnest portions of the thin film are most active especially when film resistivity is large. It is the thinnest portions which have the least curvature.

The expression, Eq. (36), shows a reasonable dependence on parameters. Previous work has indicated that a large value of the Hamaker constant promotes evaporation, presumably, because a stronger disjoining pressure pumps more liquid to the contact line region. A higher heat of vaporization Δh_m is correlated with improved performance. Thermal conductivity has a similar effect. This is not surprising since the resistance of the film to thermal conduction is assumed to be very important in the deviation of Eq. (36). Viscosity has a detrimental effect. Lubrication flow, a viscous flow, involves large

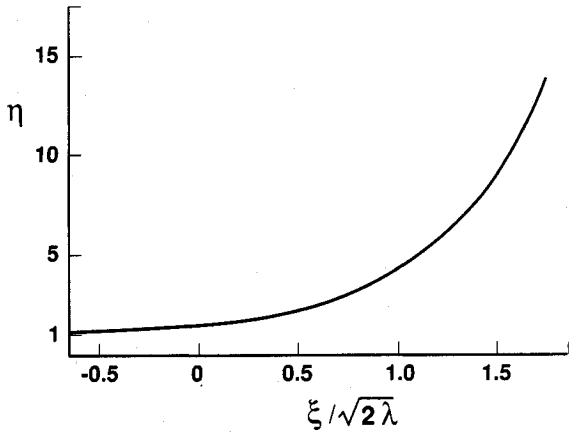

Fig. 5 Film profile for large λ (λ greater than 10, approximately).

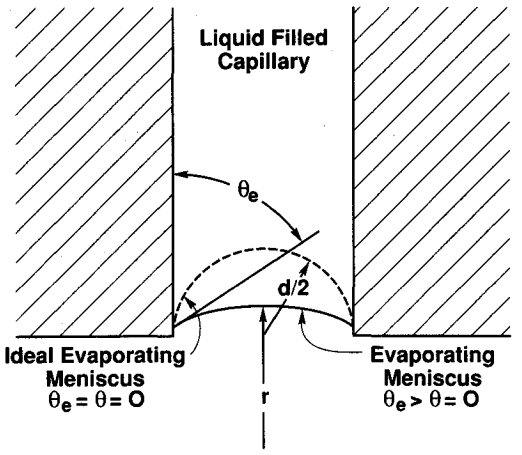

Fig. 6 Evaporating meniscus model profile.

pressure decreases which hinder evaporation. The parameter a indicates the magnitude of the response of evaporation to the degree of superheating. The parameter b indicates the propensity of the hindrance of evaporation due to the disjoining pressure. Therefore, the dependence of Q_t on a and b is plausible. Finally, we note that the elevation of the substrate temperature improves the total heat uptake. However, we do not expect the large λ solution to yield a high heat flux. For Case 1, ΔT is 5.3 $(10^{-3})°$ C and λ is 0.041, according to Eqs. (11) and (13) λ is equal to 10 only if ΔT is 3.6 $(10^{-10})°$ C. The choice of 10 is an estimate based on Eq. (A.10). Such a film would be quite thick, δ_0 would be about 1 μm, and the disjoining pressure would be virtually nonexistent.

The analysis may be related to the effective contact angle, θ_e in Fig. 6, due to evaporation by constructing an engineering model of the evaporating thin film. The thin film is assumed to consist of two parts. The thinner part is governed by disjoining pressure and is analyzed in this paper. The thicker part is a capillary meniscus which has no appreciable pressure change. Evaporation is assumed to occur only in the thinner part. Furthermore the thinner part of the film is taken to be so thin that insulation effects, $\lambda\eta$, are negligible. Therefore, the solution outlined in Eqs. (29) through (32) may be used. The two parts of the film meet smoothly so that the slope of the capillary meniscus very near the solid is equal to the slope of the disjoining pressure film. This slope is related to the integral heat sink through Eq. (32). In this way, the effective contact angle, θ_e, is related to the integral heat sink. This model is certainly an approximation. We expect a transition region between the capillary meniscus and the thinner part of the film in which both effects are important. We expect evaporation in this transition region and we expect the slope of the film to increase, therefore, the relationship between the slope and the integral heat sink is approximate. Although we do not know the accuracy of the approximation, the additional insight gained is significant.

In particular, the effective contact angle, θ_e, is related to the dimensional slope through the inverse tangent

$$\theta_e = \tan^{-1}\left(\frac{1}{3}\frac{\delta_0}{x_0}\frac{W}{u}\exp\left(\frac{1}{18}\left(\frac{W}{u}\right)^2 + \frac{1}{3}\right)\right) \tag{42}$$

According to this equation, the effective contact angle increases with increases in the integral heat sink. The contact angle is relevant because it affects the radius of curvature of a meniscus in a circular pore. For a given pore the radius of curvature, r, is larger if the contact angle θ_e is larger. Specifically,

$$r = d/(2\cos\theta_e) \tag{43}$$

where d is the diameter of the pore. In a passive cooling device the driving force for fluid flow is the Laplace pressure change at the meniscus. A larger value of r due to a change in θ_e translates to a smaller driving force for flow. Therefore, a larger value of the integral heat sink may hinder the flow of liquid to the interline.

Acknowledgment

This material is based on work supported by the Aero Propulsion Laboratory, Air Force Wright Aeronautical Laboratory, Aeronautical Systems Division (AFSC), United States Air Force, Wright-Patterson AFB, Ohio 45433-6563 under contract F33615-88-C-2821. The U.S. Government is authorized to reproduce and distribute reprints for governmental purposes notwithstanding any copyright notation. Any opinions, findings, and conclusions or recommendations expressed in this publication are those of the author and do not necessarily reflect the view of the U.S. Air Force.

Appendix A: Development of Equation (27)

The governing Eq. (23) is

$$\frac{d}{d\xi}\left(\frac{1}{\eta}\frac{d\eta}{d\xi}\right) = \frac{1}{1+\lambda\eta}\left(1 - \frac{1}{\eta^3}\right) \tag{A1}$$

The presence of the η^3 term suggests the transformation

$$u = \eta^3 \tag{A2}$$

This is only useful in the special case of λ equal zero. The transformed equation is

$$\frac{1}{3}\frac{d}{d\xi}\left(\frac{1}{u}\frac{du}{d\xi}\right) = \frac{1}{1+\lambda u^{1/3}}\left(1 - \frac{1}{u}\right) \tag{A3}$$

As mentioned in the text, this is invariant with respect to translation in ξ, that is, if we replace ξ with ϕ such that

$$\phi = \xi - c \tag{A4}$$

where c is some constant, the differential equation for $u(\phi)$ is identical to (A.3). Therefore, following Bluman and Cole,[13] we introduce the transformation

$$W = \frac{du}{d\xi} \tag{A5}$$

The chain rule implies

$$\frac{d}{d\xi} = \frac{du}{d\xi}\frac{d}{du} = W\frac{d}{du} \tag{A6}$$

Therefore, Eq. (A.3) may be rewritten

$$\frac{1}{3} W \frac{d}{du}\left(\frac{W}{u}\right) = \frac{1}{1 + \lambda u^{1/3}}\left(1 - \frac{1}{u}\right) \tag{A7}$$

or

$$\frac{1}{3}\frac{W}{u}\frac{d}{du}\left(\frac{W}{u}\right) = \frac{1}{1 + \lambda u^{1/3}}\left(1 - \frac{1}{u}\right)\frac{1}{u} \tag{A8}$$

This may be integrated to yield

$$\frac{1}{6}\left(\frac{W}{u}\right)^2 = \int \frac{1}{1 + \lambda u^{1/3}}\left(1 - \frac{1}{u}\right)\frac{1}{u}\, du \tag{A9}$$

The integral is simpler if u is eliminated in favor of η with Eq. (A.2). We find

$$\frac{1}{18}\left(\frac{W}{u}\right)^2 = \int \frac{d\eta}{\eta(1 + \lambda\eta)} - \int \frac{d\eta}{\eta^4(1 + \lambda\eta)} \tag{A10}$$

The integrals were solved by the method of "partial fractions" for the expression (27). The farfield condition implies that

$$\frac{W}{u} \to 0 \tag{A11}$$

as

$$\eta \to 1 \tag{A12}$$

This fixes the constant of integration.

References

[1]Derjaguin, B. V., and Zorin, Z. M., "Optical Study of the Adsorption and Surface Condensation of Vapors in the Vicinity of Saturation on a Smooth Surface," *Proceeding 2nd International Congress on Surface Activity (London)*, Butterworths, London, Vol. 2, pp. 145–152, 1957.

[2]Derjaguin, B. V., Nerpin, S. V., and Churayev, N. V., "Effect of Film Transfer upon Evaporation of Liquids from Capillaries, *Bulletin Rilem*, No. 29, December 1965, pp. 93–98.

[3]Potash, M., Jr., and Wayner, P. C., Jr., "Evaporation from a Two-Dimensional Extended Meniscus," *International Journal of Heat Mass Transfer*, Vol. 15, 1972, pp. 1851–1863.

[4]Miller, C. A., "Stability of Moving Surfaces in Fluid Systems with Heat and Mass Transfer," *American Institute of Chemical Engineers Journal*, Vol. 19, No. 5, 1973, pp. 909–915.

[5]Wayner, P. C., Jr., Kao, Y. K., and LaCroix, L. V., "The Interline Heat Transfer Co-efficient of an Evaporating Wetting Film," *International Journal of Heat Mass Transfer*, Vol. 19, 1976, 487–492.

[6]Holm, F. W., and Goplen, S. P., "Heat Transfer in the Meniscus Thin-Film Region," *Transactions of the American Society of Mechanical Engineers Journal of Heat Transfer*, Vol. 101, 1979, pp. 543–547.

[7]Moosman, S., and Homsy, G. M., "Evaporating Menisci of Wetting Fluids," *Journal of Colloid Interface Science*, Vol. 73, No. 1, 1980, pp. 212–223.

[8]Parks, C., and Wayner, P. C., Jr., "Surface Shear Near the Contact Line of a Binary Evaporating Curved Thin Film," *American Institute of Chemical Engineers Journal*, Vol. 33, No. 1, 1987, pp. 1–10.

[9]Mirzamoghadam, A., and Catton, I., "A Physical Model of the Evaporating Meniscus," *American Society of Mechanical Engineers Journal of Heat Transfer*, Vol. 110, 1988, pp. 201–207.

[10]Das, S., and Gaddis, J. L., "Pressure Distribution near an Evaporating Contact Line," *Nonequilibrium Transport Phenomena* edited by F. Dobran, S. G. Bankoff, J. C. Chen, and M. S. El-Genk, HID-Vol. 77, American Society of Chemical Engineers, New York, NY, 1987, pp. 17–21.

[11]Wayner, P. C., Jr., and Schonberg, J., "Heat Transfer and Fluid Flow in an Evaporating Extended Meniscus," *Proceedings of 9th International Heat Transfer Conference*, edited by G. Hestroni, Vol. 4, Hemisphere Publishing Corp., New York, 1990, pp. 228–234.

[12]Burelbach, J. P., Bankoff, S. G., and Davis, S. H., "Nonlinear Stability of Evaporating/Condensing Liquid Films," *Journal of Fluid Mechanics*, Vol. 195, 1988, pp. 463–494.

[13]Schrage, R. W., *A Theoretical Study of Interphase Mass Transfer*, Columbia University Press, New York, 1953.

[14]Wayner, P. C., Jr., "A Dimensionless Number for the Contact Line Evaporative Heat Sink," *Journal of Heat Transfer*, Vol. 111, 1989, pp. 813–815.

[15]Bluman, G. W., and Cole, J. D., *Similarity Methods for Differential Equations*, Springer-Verlag, Berlin, 1974.

[16]Truong, J. G., and Wayner, P. C., Jr., "Effect of Capillary and van der Waals Dispersion Forces on the Equilibrium Profile of a Wetting Fluid: Theory and Experiment," *Journal of Chemical Physics*, Vol. 87, No. 7, 1987, pp. 4180–4188.

[17]Schonberg, J. A., and Wayner, P. C., Jr., in preparation, 1990.

[18]Cook, R., Tung, C. Y., and Wayner, P. C., Jr., "Use of Scanning Microphotometer to Determine the Evaporative Heat Transfer Characteristics of the Contact Line Region," *Journal of Heat Transfer*, Vol. 103, 1981, pp. 325–330.